# Kardar-Parisi-Zhang interfaces bounded by long-ranged potentials

Omar Al Hammal,[1] Francisco de los Santos,[1] Miguel A. Muñoz,[1] and Margarida M. Telo da Gama[2]
[1]*Departamento de Electromagnetismo y Física de la Materia and Instituto Carlos I de Física Teórica y Computacional, Universidad de Granada, Fuentenueva s/n, 18071 Granada, Spain*
[2]*Centro de Física Teórica e Computacional e Departamento de Física da Faculdade de Ciências da Universidade de Lisboa, Avenida Professor Gama Pinto, 2, P-1649-003 Lisboa Codex, Portugal*
(Received 7 March 2006; published 26 July 2006)

We study unbinding transitions of a nonequilibrium Kardar-Parisi-Zhang interface in the presence of long-ranged substrates. Both attractive and repulsive substrates, as well as positive and negative Kardar-Parisi-Zhang nonlinearities, are considered, leading to four different physical situations. A detailed comparison with equilibrium wetting transitions as well as with nonequilibrium unbinding transitions in systems with short-ranged forces is presented, yielding a comprehensive picture of unbinding transitions and of their classification into universality classes. These nonequilibrium transitions may play a crucial role in the dynamics of the wetting or growth of systems with intrinsic anisotropies.

DOI: 10.1103/PhysRevE.74.011121 PACS number(s): 02.50.Ey, 05.50.+q, 64.60.−i

## I. INTRODUCTION

Spatial constraints in systems where two (or more) bulk phases coexist may lead to wetting transitions. This is the case, for example, of confined fluids where one of two coexisting equilibrium phases (the liquid, say) is in contact with a substrate with an interface separating it from the second phase (the gas) at infinity. The liquid *does not wet* the substrate if the thickness of the liquid film is finite (there is a microscopic quantity of liquid). On the other hand, the substrate is *wet* if there is a macroscopically thick liquid film on it. A wetting transition is said to occur when the substrate changes from not being wet by the liquid to being wet. Typically, two types of wetting transitions can be considered: by increasing the temperature at bulk coexistence one may find either *critical wetting* or a discontinuous transition; by varying the chemical potential while the temperature is fixed above the wetting transition temperature one finds a *complete wetting* transition, at bulk coexistence. Under equilibrium conditions, a completely analogous transition (often called drying) may occur when the substrate preferentially adsorbs the gas phase [1].

Effective interfacial potentials are useful coarse-grained models that have played a key role in understanding a large variety of equilibrium wetting problems [1,2]. These potentials $V(h)$ are functionals of the interfacial height (measured from the substrate), $h(\mathbf{x})$. In this framework, wetting transitions are described as the unbinding of the (say, liquid-vapor) interface from the substrate, with the effective binding potential determined by the microscopic forces between the constituents of the substrate and those of the bulk phases. Typically, exponentials and power-law decaying potentials $V(h)$ have been considered for systems dominated by short-ranged and long-ranged forces, respectively.

There exists a large amount of phenomena describable in terms of equilibrium wetting, either under short-ranged or under long-ranged interactions, while it has only recently been recognized that nonequilibrium effects, such as anisotropies in the interface growing rules, may play a crucial role in describing some experimental situations. Within this perspective, short-ranged *nonequilibrium wetting* has been studied [3,4] and some interesting novel phenomenology has been elucidated (see [5] for recent reviews). In particular, liquid-crystals [6], molecular-beam epitaxial systems, such as GaAs [7], or materials exhibiting Stranski-Krastanov instabilities [8] appear to be good candidates to require a nonequilibrium wetting description. However, some of these systems, as well as many others not enumerated, might include effective long-ranged substrate-interface effects as also occurs in the equilibrium case.

Our goal in this paper is to fill this gap by providing a general and systematic theory of nonequilibrium wetting under the presence of effective long-ranged interactions. First, we briefly review the equilibrium situation to set up the theoretical framework and, afterwards, generalize it to embrace nonequilibrium situations.

In equilibrium, two types of analytical approaches are available: static studies based on the ensemble theory [1] and dynamical, stochastic approaches that allow investigating relaxational aspects. The second approach is amenable to nonequilibrium extensions and is the one we employ. Thus, consider the simple Edwards-Wilkinson dynamics [9] subject to a bounding force (i.e., the derivative of the bounding potential) [10]:

$$\partial_t h(\mathbf{x},t) = \nabla^2 h + a - \frac{\partial V(h)}{\partial h} + \sigma\eta(\mathbf{x},t). \tag{1}$$

This includes (i) the usual diffusion term, computed as minus the derivative of a standard surface-tension term, (ii) the driving force $a$, related to the chemical potential difference between the two phases, (iii) the Gaussian white noise $\eta(\mathbf{x},t)$, and (iv) the bounding force, which may derive from a short-ranged potential

$$V(h) = \frac{b}{p}e^{-ph} + \frac{c}{q}e^{-qh} \tag{2}$$

or from a long-ranged one

 

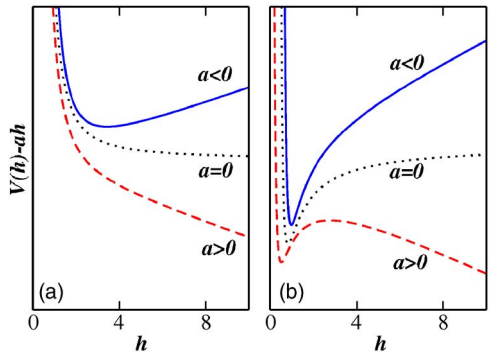


FIG. 1. (Color online) Effective potentials as derived from Eq. (3) in the pinned ($a<0$) and the depinned ($a>0$) phases and at coexistence ($a=0$). (a) Repulsive walls ($b,c>0$) and (b) attractive walls ($b<0$, $c>0$).

$$V(h) = \frac{b}{ph^p} + \frac{c}{qh^q}, \tag{3}$$

where $b$, $c>0$, and $p<q$ are parameters. This last form, Eq. (3), is known to be the correct functional form for systems where the molecules interact through van der Waals forces [11].

By varying the chemical potential $a$, one controls the average interfacial distance from the wall: small for $a<a_c$ (nonwet phase), large for $a \approx a_c$, and increasing steadily with time for $a>a_c$ (wet phase); i.e., the system exhibits an unbinding transition at $a=a_c$. The interface potentials $V(h)$ are, in all cases, harshly repulsive at small $h$ to model the impenetrability of the substrate. The parameter $b$ vanishes linearly with the temperature, at the (mean-field) critical wetting temperature, and represents the affinity or preference of the substrate for one of the bulk phases (usually the liquid). We consider three distinct situations (see Fig. 1).

(i) *Repulsive potential: complete wetting*. If $b>0$, the potential describes the presence of a bounding substrate alone. In this case, the broken symmetry induced by the substrate leads to the divergence of the average position of the interface, at coexistence, $a_c=0$: i.e., the system undergoes a *complete wetting* transition.

The latter is described by Eq. (1) with the potential taken from Eq. (2). Two different regimes depending on the value of $p$ have been reported: for $p<2$ mean-field scaling holds and $\langle h \rangle \sim t^{1/(p+2)}$, while if $p>2$ fluctuations take over and the velocity is controlled by the intrinsic roughness of a free Edwards-Wilkinson, leading to a fluctuation-dominated regime characterized by $\langle h \rangle \sim t^{1/4}$ (0, or logarithmic growth for two-dimensional interfaces) [12]. These results are derived in a formal way and extended in the Appendix.

(ii) *Attractive potential: first-order unbinding*. For $b<0$, by contrast to the complete wetting case, the surface does not promote the growth of the liquid phase and consequently there is no wetting phase even at bulk coexistence, $a=0$. $V(h)$ exhibits a local minimum near the substrate, which binds the interface in the presence of thermal fluctuations, and the width of the wetting layer is finite (microscopic) at $a=0$. We may, however, observe a first-order unbinding transition that occurs as $a$ changes from positive (stable bulk liquid) to negative (stable bulk gas) values.

(iii) *Critical wetting*. At a particular value of $b=b_c$ ($b_c=0$ in the mean field but more generally $b_c$ is small and negative) critical wetting may be observed, with a characteristic nontrivial phenomenology. This situation requires the fine-tuning of two independent parameters ($b=b_w$, $a=a_c$). This critical transition is more difficult to treat theoretically and less likely to be found in real systems and will not be discussed in this paper.

The best way to extend equilibrium approaches to more general, nonequilibrium, situations is to consider the simplest and widely studied nonequilibrium extension of the Edwards-Wilkinson equation—i.e., the Kardar-Parisi-Zhang (KPZ) [9,13] interfacial dynamics [14]—in the presence of effective bounding potentials, as the ones we have described before. This strategy has been followed in a series of recent papers for systems with short-ranged (attractive and purely repulsive) potentials [5] and will be extended in the present work to the case of long-ranged potentials. We will discuss the phase diagrams for both purely repulsive and attractive potentials, paying special attention to criticality and to the comparison with equilibrium wetting and nonequilibrium short-ranged unbinding. We will focus on one-dimensional interfaces (separating two-dimensional bulk phases) and mention briefly two-dimensional interfaces in the Conclusions.

The paper is organized as follows. In Sec. II we introduce the nonequilibrium unbinding model. In Sec. III, we review known results for nonequilibrium short-ranged unbinding. Section IV contains the main body of the paper, including both analytical and numerical results for purely repulsive and attractive potentials. Finally, the main conclusions are presented together with a discussion of our results.

## II. NONEQUILIBRIUM LONG-RANGED UNBINDING: THE MODEL

Our model consists of a KPZ nonequilibrium interface [9,13] in the presence of a long-ranged, bounding potential, Eq. (3),

$$\partial_t h = \nabla^2 h + \lambda(\nabla h)^2 + a + \frac{b}{h^{p+1}} + \frac{c}{h^{q+1}} + \sigma\eta(\mathbf{x},t), \tag{4}$$

where $\lambda \neq 0$ is the coefficient of the nonlinear KPZ term, the only new ingredient added to the equilibrium wetting Langevin equation (1).

Note that in equilibrium the time-dependent probability distribution $P(h,t)$ is symmetric for the free interface, and therefore it does not make any difference which side faces the substrate. By contrast, under nonequilibrium conditions, owing to the $h \to -h$ asymmetry of the KPZ equation, it depends on the sign of $\lambda$ that the substrate probes either one tail or the other of a KPZ probability distribution that is no longer symmetric. Thus, for a given bounding potential two different situations must be considered. Therefore, we will investigate systems with positive and negative values of $\lambda$ (without loss of generality we take $\lambda = \pm 1$) and with both attractive ($b<0$) and repulsive ($b>0$) potentials; i.e., we

consider *four distinct cases*. The focus is mainly on one-dimensional interfaces.

For *analytical studies* we employ simple power-counting arguments to establish the relevance or irrelevance of the new terms at the equilibrium renormalization-group fixed points. These will be combined with heuristic and scaling arguments to relate the emerging critical behavior to equilibrium wetting and short-ranged nonequilibrium unbinding.

For *numerical studies*, we consider one-dimensional discretizations of Eq. (4). As direct integrations of KPZ-like equations are known to be plagued with numerical instabilities [15], we resort to the exponential or Cole-Hopf transformation $n=\exp(\pm h)$, which leads to well-behaved, numerically tractable, Langevin equations with multiplicative noise [5,16]. In order to integrate these equations we employ a recently proposed efficient numerical scheme [17], specifically designed to deal with stochastic equations with nonadditive noise. More than just a useful technical trick, this transformation has an interesting physical motivation, as we discuss next. For negative values of $a-a_c$, the average interfacial height $\langle h\rangle$ (thickness of the liquid film) may be large but finite, and the interface fluctuates around its average position occasionally touching the substrate. As the interface moves to infinity when $a\to a_c$, its average height grows (i.e., the liquid film completely wets the substrate), thereby suppressing contact (dry) sites. An appropriate order-parameter (OP) for the unbinding transition is the number of contact (dry) sites [3,18] or, equivalently, the surface order parameter [19]. This OP is finite and positive when the interface is bound and vanishes at the unbinding transition. The variable $\langle n\rangle=\langle\exp(-h)\rangle$, which vanishes exponentially far from the wall, is an adequate mathematical representation of such an OP (though not the only one).

The main goal of our study is the description of the scaling behavior of the OP. $\langle n\rangle$ is expected to obey simple scaling near the critical point for sufficiently large times $t$ and large system sizes $L$. Denoting $\delta a=|a-a_c|$,

$$\langle n(\delta a,t,L)\rangle = L^{-\beta_{OP}/\nu}\langle n(L^{1/\nu}\delta a,L^{-z}t)\rangle, \tag{5}$$

while right at the transition $\langle n(\delta a=0,t)\rangle\sim t^{-\beta_{OP}/\nu z}\sim t^{-\theta_{OP}}$ and therefore $\langle n(\delta a,t=\infty)\rangle\sim\delta a^{\beta_{OP}}$, where the critical exponents were introduced following standard nomenclature. Analogously, for the interfacial height we can define $\langle h\rangle\sim\delta a^{-\beta_h}$ and $\langle h(\delta a=0,t)\rangle\sim t^{\beta_h/\nu z}\sim t^{\theta_h}$, although in terms of $h$ a single universality class, with exponents related to the free KPZ [16], is observed for both signs of $\lambda$. Determining all of these critical exponents by the aforementioned techniques will allow us to assign the emerging critical behavior to specific universality classes, providing a comprehensive classification of nonequilibrium unbinding transitions in the presence of long-ranged forces.

Before proceeding to the presentation of our results, we notice that it is expected that the behavior for short-ranged interactions is recovered in the large-$p$ limit of the long-ranged ones. Next, a brief review of the former is provided.

## III. BRIEF REVIEW OF NONEQUILIBRIUM SHORT-RANGED UNBINDING

The KPZ equation with exponential bounding potentials is

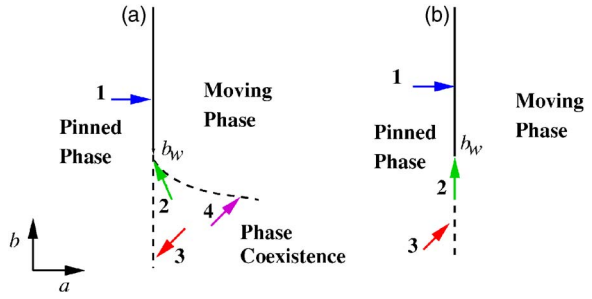


FIG. 2. (Color online) Phase diagrams for $\lambda<0(a)$, $\lambda>0(b)$. Paths labeled 1 correspond to nonequilibrium complete wetting transitions; 2, critical or first-order unbinding transitions (not studied); 3, first-order unbinding transitions; 4, unbinding transition in the directed percolation universality class. For $\lambda<0$ and $b<b_w$ (attractive substrates), two-phase coexistence is observed in the area delimited by the two lines.

$$\partial_t h = \nabla^2 h + \lambda(\nabla h)^2 + a + be^{-ph} + ce^{-qh} + \sigma\eta, \tag{6}$$

with $q>p>0$. The results for the four possible physical situations are the following.

### A. Repulsive wall and $\lambda<0$

If $\lambda<0$ (we set $\lambda=-1$), the change of variables $n=\exp(-h)$ transforms Eq. (6) (with $c=0$) into

$$\partial_t n = \nabla^2 n - an - bn^{1+p} + n\sigma\eta. \tag{7}$$

This describes complete wetting transitions [along path 1 in Fig. 2(a)] characterized by (see [5]) a dynamic exponent $z=3/2$, identical to KPZ, $\nu=1/(2z-2)=1$, and nontrivial exponents $\beta_{OP}$ and $\theta_{OP}$, which were determined by simulations. The exponents for $h$ have been measured also, and the transition was shown to be in the *multiplicative noise 1* (MN1) universality class: $\beta_{OP}\approx 1.78$, $\theta_{OP}\approx 1.18$, $\theta_h\approx 0.33$, and $\beta_h\approx 1/2$ in $d=1$ [5].

### B. Repulsive wall and $\lambda>0$

As for the $\lambda<0$ case, it is more convenient [20] to use the transformation $n=\exp(+h)$, leading to

$$\partial_t n = \nabla^2 n + an + bn^{1-p} + n\sigma\eta. \tag{8}$$

This equation describes the transition along path 1 in Fig. 2(b). Numerical estimates for the associated universality class have been recently obtained from this (non-order-parameter) Langevin equation [20]. By measuring the order parameter $m=\langle 1/n\rangle$ (which vanishes at the transition), the following set of exponents was obtained: $\theta_{OP}\approx 0.22$, $\beta_{OP}\approx 0.32$, different from MN1 and $\theta_h\approx 0.33$, $\beta_h\approx 0.5$, $z=3/2$, and $\nu=1$, in line with the corresponding exponents of the MN1 class [3,20,21]. This universality class is known as *multiplicative noise 2* (MN2). A detailed discussion of the differences between the MN2 and MN1 universality classes may be found in [5].

Note that, apart from the signs, the difference between Eqs. (7) and (8) is in the leading power of $n$. It is possible, however, to summarize these two Langevin equations in

$$\partial_t n = \nabla^2 n + \alpha a n + \alpha b n^\gamma + n\sigma\eta, \tag{9}$$

with $\alpha=\lambda/|\lambda|$ and $\gamma=1-\alpha p$. Then $\alpha>1$ and $\alpha<1$ correspond, respectively, to the MN1 and MN2 universality classes. In the first case the leading power for large values of $n$ is the nonlinear term while this role is taken by the linear term in the second case. The transition at the boundary $\gamma=1$ ($p=0$) is obviously discontinuous, as both terms are linear and there is no saturating term.

In MN1 the order parameter is $n$, while in the MN2 case, it is $m=1/n$. In both cases $a$ is the control parameter.

### C. Attractive wall and $\lambda<0$

For attractive walls, $b<0$, a positive value of $c$ is required for stability, for any value of $\lambda$. In systems with $\lambda<0$ [see Fig. 1(a)], a new phenomenology including a broad coexistence region and a directed-percolation unbinding transition emerges [3,5,22,23]. In the broad-coexistence region the stationary solution is either bound or unbound depending on the initial conditions [4,5]. Such a region is delimited on the right (where the bound phase loses stability) by a directed percolation transition, where the scaling properties are controlled by the effective dynamics of the particlelike interface-surface contact points (i.e., points trapped in the potential well). Its leftmost border corresponds to the abrupt (discontinuous) binding of initially unbound interfaces. Again we refer the reader to [5] for a detailed discussion and to [23] for a review of generic phase coexistence in nonequilibrium systems.

### D. Attractive wall and $\lambda>0$

For $\lambda>0$ [see Fig. 1(b)] a first-order transition separates bound from unbound phases (akin to the equilibrium discontinuous transition for attractive walls). No broad coexistence region or directed percolation transition exists in this case.

## IV. NONEQUILIBRIUM LONG-RANGED UNBINDING: RESULTS

We are now set to discuss the long-ranged nonequilibrium problem described by Eq. (4). There is a singularity at $h=0$, and thus only positive values of $h$ are allowed (mimicking the impenetrability of the substrate). As before, if $b>0$, we take $c=0$ for simplicity. Proceeding as in the short-ranged nonequilibrium case, we perform the change of variables $n=\exp(\alpha h)$, with $\alpha=\lambda/|\lambda|$, in Eq. (4), obtaining

$$\partial_t n = \nabla^2 n + \alpha a n + \alpha b \frac{n}{|\alpha \ln(n)|^{1+p}} + n\sigma\eta, \tag{10}$$

where a term $+\alpha c n/|\alpha \ln(n)|^{1+q}$ has to be added when $b<0$. As before, for positive $\lambda$ ($\alpha=1$), the order parameter is $m=1/n$, while for $\lambda<0$ the order parameter is $n$ itself. Note also that as there is a singularity at $n=1$ [inherited from the singularity at $h=0$ in Eq. (4)], for $\lambda>0$, where $n$ diverges at the transition and the initial condition is fixed at $n(x)>1\,\forall\, x$, while for $\lambda<0$, where $n$ vanishes at the transition, $0<n(x)<1\,\forall\, x$ is taken. The deterministic one-site terms of Eq. (10) may be written as minus the derivative of a potential $U(n)$, which is depicted in Fig. 3.

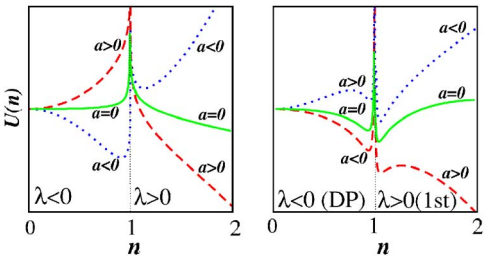


FIG. 3. (Color online) Effective potentials in terms of $n$ obtained from the numerical integration of the interaction part of Eq. (10). Left and right panels correspond to, respectively, repulsive ($b=1$) and attractive ($b=-1$) interactions. For both $b$ we show results for negative and positive $\lambda$ and different values of $a$ corresponding to the bound and unbound phases, as well as at coexistence. Note that for $\lambda<0$ ($>0$) the unbound phase corresponds to a minimum of $n$ at 0 ($\infty$). Transitions for attractive walls can be either first order or continuous (directed percolation).

It is instructive to compare this model with the two universality classes reported for nonequilibrium short-ranged wetting—i.e., MN1 and MN2. In fact, it is expected that, in the limit of sufficiently large $p$, the power-law force yields the same dynamics as short-ranged (exponential) forces. Thus, for $\lambda<0$ and large $p$ we anticipate MN1 behavior while MN2 scaling should obtain when $\lambda>0$, in the same limit.

### A. Analytic results

In an early work the KPZ nonlinearity was argued to be irrelevant above the (mean-field) wetting temperature $b=b_w=0$ and an equilibrium (complete) wetting transition was predicted to occur as $a\to a_c$, at constant $b>b_w$, for any $\lambda$ [24] (transitions along path 1 in Fig. 2). In the following we show that such a prediction is untenable and that the nonequilibrium term leads to new physics.

Let us start by employing naive power counting arguments, based on equilibrium scaling, to decide whether $\lambda$ is a relevant or an irrelevant perturbation, at the mean-field fixed point and at the fluctuation one. In order to do that, we first fix $\lambda=0$ in Eq. (4). If $b>0$, then the upper critical dimension depends only on the repulsive part of the potential and is $d_c(p)=2p/(2+p)$ [25,26], as shown in the Appendix. Now, from dimensional analysis, $[\lambda]=L^{-1+d/2}$. Upon evaluating it at $d_c(p)$ one finds $[\lambda]=L^{-2/(2+p)}$ which, in terms of momenta, has a positive dimension for any value of $p$. Therefore, the KPZ nonlinearity is relevant at the mean-field equilibrium wetting transition.

Relevancy at the fluctuating regime fixed point is proved using the known one-dimensional scaling dimension of the field $[h]\sim t^{1/4}\sim L^{1/2}$ at the fluctuation-dominated fixed point (see the Appendix). Then, it follows that $[\lambda]=L^{-(d+1)}$, implying that $\lambda$ is strongly relevant in any space dimension. To be rigorous we would need to include perturbative corrections generated by the new nonlinear term proportional to $\lambda$, but even without computing these, one can say that it is very

unlikely that such corrections reverse the strong lowest-order relevancy of $\lambda$. The relevancy of $\lambda$ is strongly supported by the results of numerical simulations of the corresponding Langevin equation as we will show next.

As in one-dimensional equilibrium interfaces, where $p=2$ separates the mean-field and the fluctuation-dominated regimes, it is easy to argue that in nonequilibrium the two regimes are separated by $p=1$. From Eq. (4) in the absence of noise, the mean-field velocity exponent at the critical point, given by $\lambda\langle(\nabla h)^2\rangle+a_c=0$, is obtained by integrating $\partial_t h \sim h^{-p-1}$ and found to be $\theta_h=1/(p+2)$. On the other hand, when noise (fluctuations) is included, the (one-dimensional) free KPZ equation has a roughening exponent of $1/3$ and, therefore, a velocity proportional to $t^{1/3}$ [9]. Which of these contributions dominates? Clearly, if $p<1$, the wall-induced velocity is larger and fluctuations give only a higher-order correction (i.e., they are irrelevant). By contrast, if $p \geqslant 1$, the effective repulsion generated by the wall (through suppression of the intrinsic interfacial roughness) controls the scaling. Thus, in nonequilibrium long-ranged wetting, $p=1$ separates the mean-field from the fluctuation-dominated regimes.

Transient effects, which are significant before the nonequilibrium interface develops its full (asymptotic) time-dependent roughness, may prevent the KPZ exponent $\theta=1/3$ from being observed, leading to an effective exponent $\theta_{eff}<1/3$. Furthermore, at short times, the interface is expected to grow with an Edwards-Wilkinson exponent $\theta=1/4$, and therefore $\theta_{eff}$ increases progressively from $1/4$ to its asymptotic KPZ value of $1/3$ in the long-time regime. Comparing these values with the wall-induced velocity exponent $1/(p+2)$, we anticipate that for potentials with $1<p<2$ severe transient effects will occur before the fluctuation-dominated scaling sets in. By contrast, for $p>2$ fluctuations dominate from the early stages of interfacial growth.

### B. Numerical results

In order to avoid numerical instabilities, typical of KPZ direct numerical integration schemes [15], we chose to study the associated multiplicative noise, Eq. (10), obtained after performing a Cole-Hopf transformation. To solve Eq. (10) efficiently we have used a recently proposed *split-step* scheme for the integration of Langevin equations with nonadditive noise [17]. In this scheme, the equation under consideration is discretized in space and time and separated into two contributions: (i) the first includes deterministic terms only and is integrated at each time step using a standard integration scheme: Euler, Runge-Kutta, etc. [27] (here we have chosen a simple Euler algorithm) and (ii) the output of the first step is used as input to integrate (along the same discrete time step) the second part which includes the noise and, optionally, linear deterministic terms. This is done by sampling the probability distribution—i.e., the solution of the Fokker-Planck equation associated with this part of the dynamics. In the case under study (noise proportional to the field), the second step can be carried out exactly. At each site, one has to sample a log-normal distribution—i.e., the solution of the Fokker-Planck equation associated with $\partial_t n = \alpha a n + \sigma n \eta$ (for more details see [28,17]). The two-step algorithm for Eq. (10) is then implemented as follows. At each site $n=n(x,t)$, we compute

$$n_1(x,t) = n + dt\left[\frac{\alpha b n}{[\alpha \ln(n)]^{1+p}} + \nabla^2_{discr} n(x,t)\right], \qquad (11)$$

where the discretized Laplacian is defined by

$$\nabla^2_{discr} n(x,t) = \frac{n(x+\Delta x,t) + n(x-\Delta x,t) - 2n(x,t)}{\Delta x^2}, \qquad (12)$$

with $\Delta x$ the space mesh and

$$n(x,t+\Delta t) = n_1(x,t)\exp(\alpha a \Delta t + \sigma \eta \sqrt{\Delta t}), \qquad (13)$$

where $\eta$ is a random variable extracted from a normal distribution with zero mean and unit variance. Note that the linear deterministic term can be included in either the first or second step or partially incorporated in both of them. For systems with $b<0$, the stabilizing term, proportional to $c$, has be to included.

We set $\sigma=1$, $\Delta x=1/\sqrt{0.1}$, and the time mesh $\Delta t=0.1$ (note that in this scheme $\Delta t$ can be taken larger than in the usual integration algorithms [17]). In some simulations we used different values of $b$, which by default was set to $b=\pm 1$. We take as initial condition $n(x,t=0)=3$ if $\lambda>0$ (recall that $n \in ]1,\infty[$) and $n=0.5$ if $\lambda<0$ ($n \in [0,1[$). Then, the dynamics is iterated by employing the two-step integration algorithm at each site and using parallel updating.

The numerical procedure is as follows. In order to determine the critical point for any set of parameters we take the system size as large as possible and look for the separatrix between upward-bending and downward-bending curves in the order parameter (either $n$ or $m=1/n$ depending on the case) versus $t$ in a double-logarithmic plot. The asymptotic value of this slope gives an estimation of $\theta_{OP}$. Also, for the same parameters, $\langle h\rangle$ grows as a power law with an exponent $\theta_h$ (bending downward and upward in the bound and the unbound phases, respectively). Generally the order parameter is more sensitive to control-parameter variations, providing the most reliable way of determining the critical point. For completeness and in order to check the validity of analytical approximations, we measure the global interface width $W$ at the transition, which is expected to grow with the KPZ exponent $\beta_W=1/3$, in the regime where it is asymptotically free.

Once the critical point is determined accurately we compute $\beta_{OP}$ and $\beta_h$ by measuring the stationary values of the order parameter and of $\langle h\rangle$ at different distances from it. A complementary approach is based on finite-size scaling analysis: the values of the order parameter and of $\langle h\rangle$, at saturation, are measured for a fixed value of $a$ as a function of system size. At the critical point these values scale with exponents $\beta_{OP}/\nu$ and $\beta_h/\nu$, respectively. In addition, the scaling of the saturation times for different system sizes allows us to determine the dynamical exponent $z$. This standard finite-size scaling analysis is not always possible (see below), and in such cases $z$ is measured through spreading-like experiments. Finally, an alternative to spreading consists in measuring the distribution of gaps between contact points

at a given time. For small gaps this function decays with an exponent $z\theta_{OP}$, giving yet another estimate of $z$ [29].

The correlation length critical exponent $\nu$ is obtained by measuring the location of the effective critical point—i.e., the value of $a$ for which the order-parameter falls below a fixed threshold, say $10^{-3}$, as a function of system size: $a_{c,eff}(L) \sim L^{-1/\nu}$. This exponent may also be determined indirectly by employing scaling relations and using the value of $\beta_{OP}/\nu$ from finite-size scaling analysis and the value of $\beta_{OP}$ obtained from direct measurements. The results of these measurements, in conjunction with the scaling laws, provide an overcomplete estimation of the set of critical exponents, which was also used to verify scaling relations.

Before discussing the differences between the various universality classes and regimes (i.e., different values of $\lambda$, $p$, and $b$) we first give an overview of the common features of all simulations.

(i) Once the KPZ equation parameters $(D, \lambda, \sigma)$ are fixed, the location of the critical point is universal, meaning that it does not depend on the details of the substrate—i.e., on the values of $b$, $c$, and $p$. The critical point is determined by the value of $a$ where the free KPZ interface changes the sign of its velocity, from positive—i.e., diverging to an unbound state—to negative, becoming bound at the wall: $a_c + \lambda\langle(\nabla h)^2\rangle = 0$. As we consider two different values of $\lambda$, $+1$ and $-1$, there are two critical points: $a_c(\lambda = \pm 1) \approx \mp 0.143668(3)$.

(ii) At the critical point, the asymptotically unbound interface is a free KPZ one, and thus $z = 3/2$ and $\beta_W = 1/3$. These values were consistently checked in all simulations [see Figs. 4(a) and 4(b)].

(iii) A simple argument, originally given in [16], predicts $\nu = 1$ for all bounded KPZ interfaces. This prediction was confirmed in all of our cases [see the inset of Fig. 4(a)].

#### *1. Repulsive walls and $\lambda > 0$*

We have to distinguish two regimes, depending on the range of the attractive substrate—i.e., the value of $p$.

*Mean-field regime*. The theoretical discussion indicates that for $p < 1$, and any sign of $\lambda$, a mean-field regime controlled by the exponents $\theta_h = 1/(p+2)$ and $\beta_h = 3/(2p+4)$ is obtained. By changing variables in a naive way a stretched exponential behavior for the order parameter is predicted. Figure 5 (and Fig. 10, below) illustrates the confirmation of these predictions (both for positive and negative $\lambda$).

*Fluctuation regime: multiplicative noise 2*. A strong-fluctuation regime is predicted for systems with $p > 1$, but as argued above, severe transient effects are expected for $2 > p > 1$. We start with the analysis of the, *a priori*, simpler $p > 2$ subregime and offer simulation results for $p = 2, 2.5, 3, 4, 7$. In all cases the order parameter was found to decay at criticality with an exponent $\theta_{OP} \approx 0.229$ while the average height diverges with $\theta_h \approx 1/3$ (see Fig. 6, data shown for $p = 2$). A standard finite-size scaling analysis can be performed (see Fig. 6), yielding $\beta_{OP}/\nu = 0.34(2)$ and $\beta_h/\nu = 0.46(2)$.

These results, together with the previously reported general ones, unambiguously place the fluctuation regime for repulsive walls with positive $\lambda$ into the MN2 universality class.

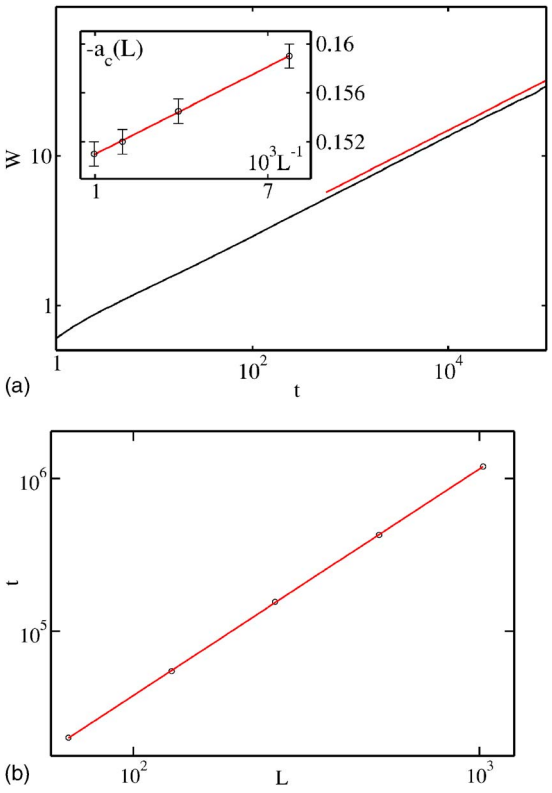


FIG. 4. (Color online) Features common to all simulations. (a) Roughness vs $t$ gives $\beta_W = 0.33(1)$; (inset) $-a_c(L)$ vs $10^3 L^{-1}$ falls on a straight line that yields $\nu \sim 1$ (data for $\lambda = -1$ and $p = 2$). (b) Saturation time vs system size leads to $z = 1.48(4)$ (data for $\lambda = 1$ and $p = 2$).

For systems with $1 < p < 2$, where strong transients are expected, after fixing $b = 1$ and running simulations up to $t = 10^6$, continuously varying power-law exponents are found

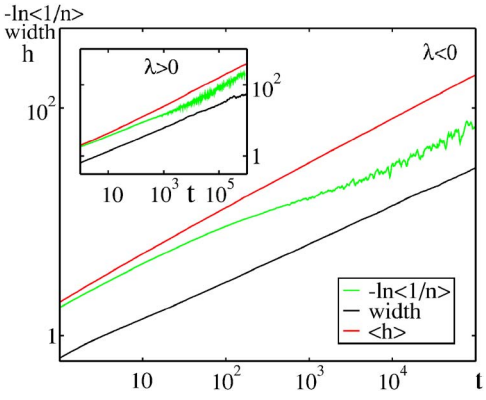


FIG. 5. (Color online) Log-log plot of the time evolution at $a_c$ of $\langle h \rangle$ (upper, red curves), $-\ln\langle n_{OP} \rangle$ (middle, green curves), and the width $w$ (lower, black curves), in the mean-field regime $p = 0.5$, for $\lambda < 0$ (main) and $\lambda > 0$ (inset). Irrespective of the sign of $\lambda$, $\langle h \rangle$ and the roughness may be fitted to a power law with the predicted exponents $\theta_h = 1/(p+2)$ and $\beta_W = 1/3$, respectively. $-\ln\langle n_{OP} \rangle$ falls on a straight line in a double logarithmic plot, confirming the stretched-exponential behavior of the order parameter.

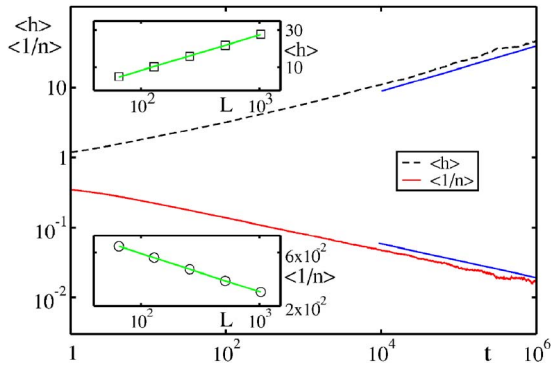


FIG. 6. (Color online) Log-log plot of the time evolution at $a_c$ of $\langle h \rangle$ (dashed, black curve) and $-\log\langle n_{OP} \rangle$ (solid, red curve) in the fluctuation regime ($p=2$) and for $\lambda > 0$. From the slopes of the straight-line fits one finds $\theta_h = 0.32(2)$ (upper curve) and $\theta_{OP} = 0.228(6)$ (lower curve). Upper inset: finite-size scaling of $\langle h \rangle$ yielding $\beta_h/\nu = 0.46(2)$. From the lower inset one obtains $\beta_{OP}/\nu = 0.34(2)$. These exponents agree with those of the MN2 universality class.

(see Fig. 7). We note, however, that these fits give effective rather than asymptotic exponents. In fact, the change in the effective exponents from the mean-field (wall-controlled) to the fluctuation (intrinsic-interface) regime is expected to occur at shorter times when the effect of the substrate is less pronounced, implying that reducing the value of $b$ decreases the crossover time. This was confirmed by simulating systems with $b=0.1$ and $b=0.05$ and observing a monotonic decrease of the effective exponents that converge to the expected asymptotic value $\theta_{OP} \approx 0.228$, $\theta_h \approx 1/3$ [see inset (a) of Fig. 7], in line with the hypothesis that the transition belongs to the MN2 universality class.

In order to check that $p=2$ is the boundary between the strong and weak transient subregimes, we have plotted in Fig. 7, inset (b), the average order parameter for systems with the same initial condition, at time $t=10^6$, and different

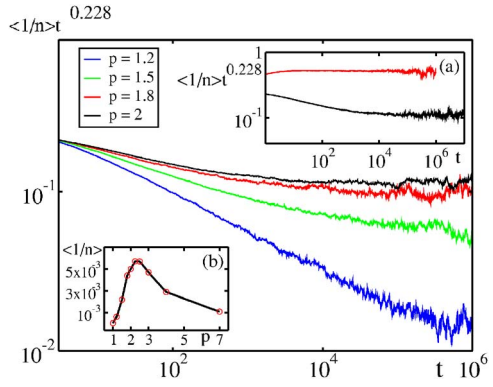


FIG. 7. (Color online) Main: order-parameter multiplied by the expected power law $t^{0.228}$. For systems with $b=1$, long transients that depend on $p$ are observed for systems with $1 < p < 2$. Inset (a): the crossover times are reduced as $b$ decreases; compare the upper, red curve for $b=0.05$ with the lower, black one for $b=1$ ($p=2$). Inset (b): order-parameter at $t=10^6$ vs $p$ ($b=1$). $p=2$ marks the boundary of the strong transient region as illustrated by the different behaviors observed above and below $p=2$.

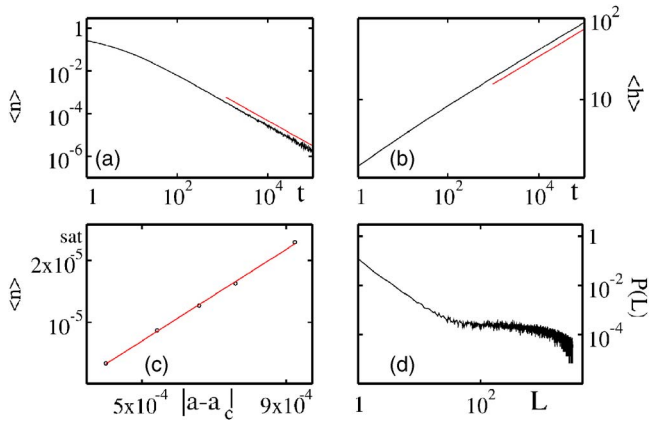


FIG. 8. (Color online) Results for $\lambda < 0$ and $p=2$. (a) Log-log plot of the time decay of the order-parameter. The straight line is a guide to the eye and has a slope $\theta_{OP} = 1.19(1)$. (b) Log-log plot of the average distance from the wall vs time, leading to $\theta_h = 0.33(1)$. (c) The scaling of the saturation value of the order parameter yields $\beta_{OP} = 1.76(3)$. (d) Log-log plot of the gap (between contact points) distribution function at $t=2^{10}$. The initial slope gives $z\theta_{OP} \approx 1.75(10)$.

values of $p$. This is a nonstationary value of the OP that is strongly affected by transients. It is clear from the figure that the behavior of the order parameter changes qualitatively at $p=2$, corroborating the result that this value of $p$ marks the boundary between the subregimes with and without severe transients.

### 2. Repulsive walls and $\lambda < 0$

*Mean-field regime*. In parallel with the positive $\lambda$ case, the results of Fig. 5 (and Fig. 10, below) show that the theoretically predicted mean-field regime is clearly observed for systems with $p < 1$.

*Fluctuation regime: multiplicative noise 1*. Again we have to distinguish two subregimes, with and without severe transients, depending on whether $p$ is larger than or smaller than 2. Simulations in the weak-transient regime were performed for $p=2$ and 3. In both of these systems the order parameter decays at criticality with an exponent $\theta_{OP} = 1.19(1)$ while the average height diverges with $\theta_h = 0.33(1)$ [see Figs. 8(a) and 8(b), data shown for $p=2$]. As was first pointed out in [29], finite-size scaling measurements are nontrivial in this case due to the presence of two different characteristic times. Namely, the correlation length reaches the size of the system at times $\sim L^z$, while the interface typically detaches from the wall at times $\sim L^{1/\theta_n}$. As the latter grows with a larger exponent for MN1, the interface detaches from the wall before it reaches the saturation regime for finite samples, rendering the evaluation of $\beta_{OP}/\nu$ and $z$ through standard finite-size scaling methods problematic. An estimation of $\beta_{OP}$ is possible by taking a large system size, $L=2^{17}$, and measuring the order-parameter stationary-state value upon approaching $a_c$. We find $\beta_{OP} = 1.76(3)$ and $\beta_h = 0.51(3)$ [see Fig. 8(c)]. $z$ is accessible through spreading experiments from an initial condition with only one active (pinned) site. The measurement of the mean-square deviation from the origin $R^2(t)$

$\approx t^{2/z}$ gives $z=1.52(5)$ (not shown). Alternatively, one can investigate the gap distribution function of the distances between neighboring contact points at a given time or, equivalently, the average size of inactive islands in the $n$ language [29]. For small gaps this function decays with an exponent $z\theta_{OP}$, and we find $z\theta_{OP}=1.75(10)$ which leads to a value of $z$ compatible with 3/2 [see Fig. 8(d)].

These results, together with the general ones, place unambiguously this fluctuation regime for repulsive walls with negative λ into the MN1 universality class.

Again, for systems with $1<p<2$, different effective exponents are obtained at a fixed maximum time for different values of $b$ (unity and smaller), confirming the existence of strong transients. Upon decreasing $b$, the influence of the wall is reduced and a behavior compatible with the MN1 class is observed: $\theta_{OP}\approx 1.19$, $\theta_h\approx 1/3$, $\beta_{OP}\approx 1.76$, and $\beta_h \approx 0.5$ (figure not shown).

### 3. Attractive wall and $\lambda<0$

The phase diagram, depicted in the left panel of Fig. 2, is similar to that found for short-ranged interactions [5]. For a fixed $b$, by varying $a$ one of two transitions may occur depending upon the initial interfacial state. Initially unbound interfaces experience an unbinding-binding transition at $a_c$ where the free-interface velocity inverts its sign (in full analogy with the previous case; see path 3 in Fig. 2). On the other hand, initially bound interfaces unbind at a different nontrivial value of $a$, denoted $a^*>a_c$, inside the free-interface unbound phase [path 4 in Fig. 2(a)]. This transition is analogous to the one observed for short-ranged forces and is expected to be controlled by the unbinding of interface sites trapped in the potential minimum. Bound sites (located around the potential minimum) are identified with particles; unbound sites are described by holes. The effective particle dynamics is very similar to that of the contact process [30] (a well-studied model known to be in the directed percolation class): an occupied site can become empty when a point is detached and can induce also the binding of a neighboring site. Furthermore, empty sites cannot become spontaneously occupied in the absence of occupied (bound) neighboring sites. Indeed, as soon as the interface is locally out of the potential well, it is pulled away from it. This corresponds to the absorbing state characteristic of the directed percolation class. Note that the statistics of the average number of such pseudoparticles is completely analogous to that of $\langle \exp(-h)\rangle$.

Before the depinning transition, typical *triangular structures* are observed, consisting of pinned sites (lying in the potential well) and depinned sites being pulled from the substrate. These triangular shapes (pyramidal in two dimensions) are similar to those in the analogous short-ranged case and are reminiscent of pyramidal mounds obtained in the nonequilibrium growing of some interfaces, such as, for instance, in the so-called Stranski-Krastanov effect [8].

Our numerical results show that this transition is controlled, as in the short-ranged case, by directed percolation critical exponents (see Fig. 9). In particular, we have determined $\beta_{OP}/\nu=0.26(2)$ and $\theta_{OP}=0.161(2)$, in excellent agreement with the one-dimensional directed percolation values.

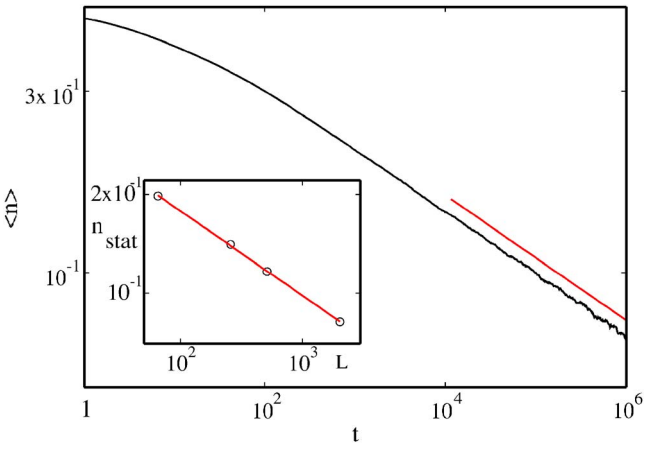


FIG. 9. (Color online) Time decay of the order-parameter at the critical point $a=0.38448$. From the slope in the log-log plot we find $\theta=0.161(2)$. Inset: finite-size scaling of the order parameter. From the slope in the log-log plot we estimate $\beta/\nu=0.26(2)$, in agreement with directed percolation values.

Let us remark that, as the bound sites remain inside the potential well and the dynamics controlling their final "escape" is likely to be insensitive to the exponential or power-law tails of the potential at large values of $h$, the parallel between this behavior and the directed-percolation transition for short-ranged forces is to be expected. Interestingly, Ginelli *et al.* investigated a lattice model of a generalized contact process with long-ranged interactions between the edges of low-density segments and found a transition in the directed percolation universality class for forces that decay sufficiently slowly and a first-order transition otherwise [31]. Clearly, in terms of $h$ this translates into a long-ranged interaction between the vertices forming the triangle bases, and it is reasonable to assume that, in turn, an effective long-ranged attraction between the substrate and interface must be obtained. In the light of these results it is reasonable to assume that both short- and long-ranged interactions in similar models will be characterized by the same behavior below $b_w$.

In the region between $a_c$ and $a^*$ one observes a generic (broad) phase coexistence: the stationary solution is either bound or unbound depending on the initial condition. Within this region, the bound phase is characterized by some bound sites trapped in the potential minimum and pseudounbound regions separating them [5]. In full analogy with short-ranged forces, close to the unbinding transition $a\lesssim a^*$ initially bound interfaces are stable owing to a mechanism that eliminates local fluctuations into the unbound phase: once formed, islands of the unbound phase rapidly transform into triangular mounds of fixed slope, which subsequently shrink from the edges.

### 4. Attractive wall and $\lambda>0$

When $\lambda>0$, the situation is rather similar to the one for equilibrium and for nonequilibrium ($\lambda>0$) short-ranged systems. At the critical value $a_c$ where the free interface inverts its velocity sign, there is a discontinuous unbinding-binding

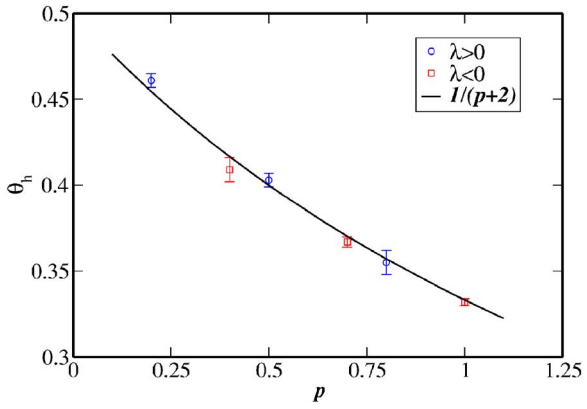


FIG. 10. (Color online) Time growth exponents $\theta_h$ in the mean-field-like regime for $\langle h \rangle$ at the critical point, as results from the discrete interfacial model. Blue circles (red squares) stand for $\lambda > 0$ ($<0$) data points, and the solid line is the predicted curve $1/(p+2)$.

transition (path 3 in Fig. 2). This value does not depend on the value of $p$, $b$, or $c$ [32].

*The multicritical point*. Finally, for either sign of λ, path 2 in Fig. 2 corresponds to a multicritical point analog to an equilibrium critical wetting transition when the critical point is approached at coexistence. Most likely, its location will not coincide with its mean-field value $b=0$, but exhibits some renormalization shift. The analysis of this multicritical point will be considered elsewhere.

### C. Discrete model

As a final check of universality issues, we simulated a discrete interfacial model, known to belong to the KPZ class, in the presence of a long-ranged substrate. The model is the same as that studied in the context of short-ranged wetting in [21]. Even if plagued with long transient effects (much larger than in the short-ranged case), all of the previously reported phase diagrams and universality classes seem to be confirmed for the different types of walls (i.e., values of $b$ and $p$) and signs of the nonlinearity. Generally, the discrete model provides slightly better results for the height variable as compared with the continuum model and worse for the order parameter.

Figure 10 displays the time growth of the mean separation $\langle h \rangle$ in the mean-field-like regime ($p<1$), for both positive and negative λ. Additionally, the ratios $\beta_{OP}/\nu=0.251(2)$ and $\theta_{OP}=0.156(2)$ were obtained for the directed percolation transition, which compares favorably with the accepted estimates 0.25208(5) and 0.1595 [33].

## V. DISCUSSION AND CONCLUSIONS

We have studied the unbinding of KPZ interfaces in the presence of limiting substrates, interacting via long-ranged potentials. This is the simplest model for interfacial effective descriptions of wetting and in general, unbinding transitions, of systems interacting through van der Waals forces under nonequilibrium conditions.

We have presented the results of systematic analytical and numerical studies of one-dimensional KPZ-like interfaces in the presence of long-ranged forces, Eq. (4), supporting the following conclusions.

(i) Repulsive interactions drive a nonequilibrium complete wetting transition for either sign of λ. This transition belongs to different universality classes depending on the strength of the repulsion—i.e., on the value of $p$ in Eq. (4) and on the sign of λ. For $p<1$ a mean-field-like regime is observed in both cases, while for $p>1$ the fluctuation regime obtains and the transition is in the multiplicative noise 1 (MN1) class for $\lambda<0$ and in the multiplicative noise 2 (MN2) for $\lambda>0$. Systems in the fluctuation regime exhibit severe crossover effects for bounding potentials with $1<p<2$. This should be contrasted with the behavior of equilibrium systems where the value of $p$ that separates the mean field from the fluctuation regimes was found to be $p=2$. More importantly, in nonequilibrium systems the symmetry of the equilibrium wetting and drying transitions is broken and the fluctuation regime of the corresponding equilibrium wetting transitions is split into two different nonequilibrium universality classes, MN1 and MN2, respectively. Our results are collected in Table I.

(ii) For attractive walls—i.e., below the critical wetting temperature—phase diagrams analogous to those of systems with short-ranged forces have been found: generic phase coexistence over a finite area limited by directed percolation and first-order boundary lines for $\lambda<0$ and a first-order phase transition from an unbound to a bound interface for $\lambda>0$. This transition should not be called "wetting" as the interface detaches below the wetting transition temperature.

The unbinding transition at the critical wetting point (which in the language of this paper corresponds to a multicritical point) requires a higher degree of fine-tuning and is therefore expected to be more difficult to observe in experimental situations. Its study is also more laborious and is deferred to future work.

For more realistic two-dimensional interfaces, corresponding to three-dimensional bulk systems, the situation is expected to be very similar: all universality classes (mean-field, multiplicative noise 1, multiplicative noise 2, and directed percolation) are expected to be substituted by their two-dimensional counterparts, with analogous phase diagrams and overall phenomenology.

We hope that the results described in this paper will help to motivate an experimental study of wetting and unbinding transitions under nonequilibrium situations. In these systems one expects to find the rich phenomenology described here and they can be used to test some of our quantitative predictions, concerning the values of the exponents and the existence of various universality classes. Liquid crystals [6], molecular-beam epitaxial systems, such as GaAS [7], claimed to grow following KPZ scaling, or materials exhibiting Stranski-Krastanov instabilities [8] appear to be good candidates that are at least worth investigating in this context. Indeed, it is rather exciting to think that nonequilibrium complete wetting exponents are measurable. This would be a way of measuring the multiplicative noise critical exponents and brings new hope of measuring directed percolation exponents in real systems [34].

TABLE I. Summary of the critical exponents in the mean-field ($p<1$) and the fluctuation ($p>1$) regimes for nonequilibrium, complete wetting transitions with long-ranged forces. To facilitate the comparison, the exponents for the MN1 and MN2 universality classes are also included ($p=\infty$). n.a., not applicable.

| | $\lambda<0$ | | | $\lambda>0$ | | |
|---|---|---|---|---|---|---|
| Exponent | $p<1$ | $p>1$ | $p=\infty$ [5] | $p<1$ | $p>1$ | $p=\infty$ [20] |
| $\theta_{OP}, \langle n\rangle \sim t^{-\theta_{OP}}$ | Stretched exp. | 1.19(1) | 1.18 | Stretched exp. | 0.228(6) | 0.229(5) |
| $\beta_{OP}, \langle n\rangle \sim \delta\alpha^{\beta_{OP}}$ | n.a. | 1.76(3) | 1.78 | n.a. | 0.34(2)[a] | 3.335(5) |
| $\theta_h, \langle t\rangle \sim t^{\theta_h}$ | $1/(p+2)$ | 0.34(1) | 0.33 | $1/(p+2)$ | 0.32(2) | 0.323(10) |
| $\beta_h, \langle h\rangle \sim \delta\alpha^{-\beta_h}$ | $3/2(p+2)$[a] | 0.51(3) | 0.5 | $3/2(p+2)$[a] | 0.46(2)[a] | 0.48(3) |
| $z, \xi \sim t^{1/z}$ | $3/2$[b] | 1.52(5) | 3/2 | $3/2$[b] | 1.48(4) | 1.46(5) |
| $\beta_W, W \sim t^{\beta_W}$ | $1/3$[b] | 0.33(1) | | $1/3$[b] | $1/3$[b] | |
| $\nu_x, \xi \sim \delta a^{-\nu_x}$ | 1[b] | 1 | 1 | 1[b] | 1[b] | 0.99(3) |

[a]Exponent from finite-size analysis or scaling relations.
[b]Estimated value from short simulations.


## ACKNOWLEDGMENTS

We acknowledge financial support from MEyC-FEDER, Project No. FIS2005-00791, and from Junta de Andalucía as group FQM-165. The "Acción Integrada hispano-portuguesa" Grant No. HP2003-0028 is also acknowledged.


## APPENDIX: BRIEF REVIEW OF EQUILIBRIUM WETTING

The action associated with Eq. (1) [26,35] (setting $c=0$) is

$$\mathcal{S}(h,\tilde{h}) = \int d^dx dt \{\tilde{h}^2 - \tilde{h}[\partial_t h - \nabla^2 h - a - bh^{-p-1}]\}, \tag{A1}$$

where $\tilde{h}$ denotes, as usual, the response field [26,35]. If one assumes first that the interaction term is the dominant one, from naive dimensional analysis, imposing $b$ to be dimensionless at the upper critical dimension and equating the dimensions of the time derivative and the potential terms, one obtains $[h]_{MF}=L^{2/(p+2)}$ and consequently, within the mean field, $\theta_h=1/(p+2)$ since time scales naively as $L^2$. The exponent values $\beta_h=1/(p+1)$ and $\nu=(p+2)/(2p+2)$ are then obtained by matching $[a]=[h]_{MF}^{-p-1}$ and by identifying $L$ with the characteristic correlation length, respectively.

On the other hand, when fluctuations (i.e., the noise term) dominate, we require the noise amplitude to be dimensionless at the upper critical dimension, which leads to $[\tilde{h}]_{FL}=L^{(2+d)/2}$, and therefore $[h\tilde{h}]=L^{-d}$, $[h]_{FL}=L^{(2-d)/2}$. From this, proceeding as before, $\theta_h=(2-d)/4$, $\nu=2/(d+2)$, and $\beta_h=(2-d)/(d+2)$. These results (which may be obtained using a number of different procedures [1,2,10,36–38]) are exact as long as $h$ and $\tilde{h}$ do not have anomalous dimensions, which has been shown to be the case [36].

The upper critical dimension is defined by $[h]_{MF}=[h]_{FL}$, which yields $d_c(p)=2p/(2+p)$. Note that for $d>d_c(p)$ the critical exponents depend on the details of the interaction (i.e., on $p$) while for $d<d_c(p)$, they depend only on $d$. In particular, in one-dimensional systems, $p=2$ marks the transition between a *mean-field regime* and a *fluctuation regime*:

(i) If $p<2$, mean-field theory is valid, and consequently $\theta_h=1/(p+2)$, $\beta_h=1/(p+1)$, $z=2$, and $\nu=1/2$.

(ii) For $p\geqslant 2$, the substrate interaction decays fast enough for the fluctuations to take over and the exponents become $p$ independent: $\theta_h=1/4$, $\beta_h=1/3$, $z=2$, and $\nu=2/3$.

Note that at the limiting value $p=2$ the exponents change continuously from the mean field to the fluctuation regime. It is also remarkable that the fluctuation regime exponents coincide with those of short-ranged equilibrium wetting (characterized by exponential bounding potentials [1]).

Until now we have considered the scaling properties of $\langle h\rangle$, but as was mentioned earlier the number of dry sites or contact points between the interface and the substrate, measured by $\langle \exp(-h)\rangle$, is known to exhibit interesting scaling behavior in wetting problems [19].

(i) For $p<2$ simple mean-field scaling holds and the $h$ distribution is a Gaussian detaching from the wall at a speed controlled by its mean value. As the interface is well described by its average position, it is expected that

$$\langle e^{-h}\rangle \sim e^{-\langle h\rangle} \sim e^{-At^{1/(p+2)}}, \tag{A2}$$

yielding a *stretched exponential* decay.

(ii) For $p>2$, $\langle a+b\exp(-h)\rangle=0$ holds in the stationary state, and therefore $\langle n\rangle \propto a$; using simple scaling, $[\exp(-h)]=[a]=[\partial_t h]\sim t^{1/4-1}$, giving $\langle \exp(-h)\rangle \sim t^{-3/4}$. This result can be derived in a number of ways, including explicit calculations for discrete models in this class [39], and remains valid for long-ranged potentials in the fluctuation regime. Note the difference between this fluctuation-induced power-law behavior and the previously reported stretched exponential behavior in the mean-field regime.

For attractive walls, $b<0$, a positive value of $c$ is required to ensure the impenetrability of the substrate (see Fig. 1). In this case it is easy to argue that the interface jumps discontinuously from a bound state (for $a<0$), localized at the minimum of $V(h)$, to an unbound state (for $a>0$) through a first-order phase transition. Clearly, in terms of the contact points $\langle \exp(-h)\rangle$, the transition is also discontinuous.

[1] S. Dietrich, in *Phase Transitions and Critical Phenomena*, edited by C. Domb and J. Lebowitz (Academic Press, New York, 1983), Vol. 12; D. E. Sullivan and M. M. Telo da Gama, in *Fluid Interfacial Phenomena*, edited by C. A. Croxton (Wiley, New York, 1986); H. Nakanishi and M. E. Fisher, Phys. Rev. Lett. **49**, 1565 (1982).

[2] D. M. Kroll, R. Lipowsky, and R. K. P. Zia, Phys. Rev. B **32**, R1862 (1985).

[3] U. Alon, M. R. Evans, H. Hinrichsen, and D. Mukamel, Phys. Rev. Lett. **76**, 2746 (1996); Phys. Rev. E **57**, 4997 (1998); H. Hinrichsen, R. Livi, D. Mukamel, and A. Politi, Phys. Rev. Lett. **79**, 2710 (1997); Phys. Rev. E **61**, R1032 (2000); **68**, 041606 (2003); J. Candia and E. V. Albano, Phys. Rev. Lett. **88**, 016103 (2002).

[4] F. de los Santos, M. M. Telo da Gama, and M. A. Muñoz, Europhys. Lett. **57**, 803 (2002); Phys. Rev. E **67**, 021607 (2003).

[5] M. A. Muñoz, in *Advances in Condensed Matter and Statistical Mechanics*, edited by E. Korutcheva and R. Cuerno (Nova Science, Commack, NY, 2004); F. de los Santos and M. M. Telo da Gamma, Trends Stat. Phys. **4**, 61 (2004).

[6] M. I. Boamfa, M. W. Kim, J. C. Maan, and Th. Rasing, Nature (London) **421**, 149 (2003).

[7] A. Ballestad, B. J. Ruck, M. Adamcyk, T. Pinnington, and T. Tiedje, Phys. Rev. Lett. **86**, 2377 (2001); H.-C. Kan *et al.*, *ibid.* **92**, 146101 (2001).

[8] V. A. Shchukin and D. Bimberg, Rev. Mod. Phys. **71**, 1125 (1999).

[9] T. Halpin-Healy and Y. C. Zhang, Phys. Rep. **254**, 215 (1995); A. L. Barabási and H. E. Stanley, *Fractal Concepts in Surface Growth* (Cambridge University Press, Cambridge, England, 1995), and references therein.

[10] R. Lipowsky, J. Phys. A **18**, L585 (1985).

[11] I. E. Dzyaloshinskii, E. M. Lifshitz, and L. P. Pitaevskii, Adv. Phys. **10**, 165 (1961).

[12] Note that for higher-dimensional interfaces, the mean-field regime dominates for any $p$, $1/(p+2)>0$, as the free fluctuations are flat, being characterized by a zero roughness exponent and a logarithmic growth in $d=2$.

[13] M. Kardar, G. Parisi, and Y. C. Zhang, Phys. Rev. Lett. **56**, 889 (1986).

[14] Another possibility (presently under study) is to analyze molecular beam epitaxy (MBE) Langevin equations (known to represent a broad family of nonequilibrium interfacial growth [9]) in the presence of bounding potentials.

[15] T. J. Newman and A. J. Bray, J. Phys. A **29**, 7917 (1996). See also C. H. Lam and F. G. Shin, Phys. Rev. E **58**, 5592 (1998).

[16] G. Grinstein, M. A. Muñoz, and Y. Tu, Phys. Rev. Lett. **76**, 4376 (1996); Y. Tu, G. Grinstein, and M. A. Muñoz, *ibid.* **78**, 274 (1997); M. A. Muñoz and T. Hwa, Europhys. Lett. **41**, 147 (1998); W. Genovese and M. A. Muñoz, Phys. Rev. E **60**, 69 (1999).

[17] See I. Dornic, H. Chaté, and M. A. Muñoz, Phys. Rev. Lett. **94**, 100601 (2005), and references therein.

[18] M. Lässig and R. Lipowsky, in *Fundamental Problems in Statistical Mechanics VIII*, edited by H. van Beijeren and M. H. Ernst (Elsevier Science, New York, 1984); Phys. Rev. Lett. **70**, 1131 (1993).

[19] R. Lipowsky, Ferroelectrics **73**, 69 (1987).

[20] O. Al Hammal, F. de los Santos, and M. A. Muñoz, J. Stat. Mech.: Theory Exp. P10013 (2005). See also [21].

[21] M. A. Muñoz, F. de los Santos, and A. Achahbar, Braz. J. Phys. **33**, 443 (2003).

[22] M. A. Muñoz and R. Pastor-Satorras, Phys. Rev. Lett. **90**, 204101 (2003).

[23] M. A. Muñoz, F. de los Santos, and M. M. Telo da Gama, Eur. Phys. J. B **43**, 73 (2005). C. H. Bennett and G. Grinstein, Phys. Rev. Lett. **55**, 657 (1985). G. Grinstein, IBM J. Res. Dev. **48**, 5 (2004); www.research.ibm.com/journal/rd/481/grinstein.pdf

[24] R. Lipowsky, in *Random Fluctuations and Pattern Growth*, edited by H. Stanley and N. Ostrowsky, Vol. 157 of *NATO Advanced Study Institute, Ser. E* (Kluwer Akademic, Dordrecht, 1988).

[25] R. Lipowsky, Phys. Rev. Lett. **52**, 1429 (1984).

[26] C. J. DeDominicis, J. Phys. (Paris) **37**, 247 (1976); H. K. Janssen, Z. Phys. B **23**, 377 (1976); P. C. Martin, E. D. Siggia, and H. A. Rose, Phys. Rev. A **8**, 423 (1973); L. Peliti, J. Phys. (Paris) **46**, 1469 (1985).

[27] M. San Miguel and R. Toral, in *Instabilities and Nonequilibrium Structures VI*, edited by E. Tirapegui and W. Zeller (Kluwer Academic, Dordrecht, 1997).

[28] The part of the Langevin equation to be integrated is written as $dn_t=an_t dt+\sigma n_t dW_t$ where $dW$ is a Wiener process. Since this is interpreted in the Stratonovich sense, we can perform the change of variables $Y_t=\ln n_t$ and obtain $dY_t=adt+\sigma dW_t$. This is a drifted Brownian motion equation whose solution is given by a normal distribution of mean $y_0+adt$ and variance $\sigma^2 dt$: $\mathrm{Prob}(Y_{t+dt}=y\,|\,Y_t=y_0)=N(y_0+adt,\sigma^2 dt)$. Reverting the change of variables, we obtain a log-normal form, which can be sampled in an exact way by taking $n[t+dt|n(t)=n_0]=n_0\exp(adt+\sigma\sqrt{dt}\,\eta)$. This expression can also be derived by changing variables in the Langevin equation, performing one time-step evolution and changing back variables.

[29] T. Kissinger, A. Kotowicz, O. Kurz, F. Ginelli, and H. Hinrichsen, J. Stat. Mech.: Theory Exp. ( 2005) P06002.

[30] H. Hinrichsen, Adv. Phys. **49**, 815 (2000).

[31] F. Ginelli, H. Hinrichsen, R. Livi, D. Mukamel, and A. Politi, Phys. Rev. E **71**, 026121 (2005).

[32] The true straight-line boundary may be easily mistaken for a temperature-dependent curve. This is due to a roughness suppression effect that effectively switches off the KPZ nonlinear term when the interfaces are initially placed close to the substrate and within the potential well. In this case, a transient renormalized $\lambda_R(b)$ may be observed that leads to an apparent temperature-dependent transition $a+\lambda_R(b)\langle(\nabla h)^2\rangle=0$.

[33] I. Jensen, J. Phys. A **32**, 5233 (1999).

[34] H. Hinrichsen, Braz. J. Phys. **30**, 69 (2000).

[35] J. Zinn-Justin, *Quantum Field Theory and Critical Phenomena* (Oxford Science, Oxford, 1989).

[36] R. Lipowsky and M. E. Fisher, Phys. Rev. B **36**, 2126 (1987).

[37] M. E. Fisher and D. S. Fisher, Phys. Rev. B **25**, 3192 (1982).

[38] D. S. Fisher and D. A. Huse, Phys. Rev. B **32**, 247 (1985).

[39] F. Ginelli and H. Hinrichsen, J. Phys. A **37**, 11085 (2004).